Position Tracking Control for an Aerial Robot Passively Tethered to an Independently Moving Platform

Marco Tognon, Antonio Franchi

Preprint version 20th IFAC World Congress, Toulouse, France (2017)

Position Tracking Control for an Aerial Robot Passively Tethered to an Independently Moving Platform ⋆

Marco Tognon * **and Antonio Franchi** *

* *LAAS-CNRS, Université de Toulouse, CNRS, Toulouse, France, (e-mail: marco.tognon@laas.fr, antonio.franchi@laas.fr).*

Abstract: We study the control problem of an aerial vehicle moving in the 3D space and connected to an independently moving platform through a physical link (e.g., a cable, a chain or a rope). The link is attached to the moving platform by means of a passive winch. The latter differs from an active winch by producing only a constant uncontrollable torque. We solve the problem of exact tracking of the 3D position of the aerial vehicle, either absolute or with respect to the moving platform, while the platform is independently moving. We prove two intrinsic properties of the system, namely, the dynamic feedback linearizability and the differential flatness with respect to the output of interest. Exploiting this properties we design a nonlinear controller able to exponentially steer the position of the aerial robot along any sufficiently smooth time-varying trajectory. The proposed method is tested through numerical simulations in several non-ideal cases.

Keywords: Aerial robot control, tethered aerial vehicles, nonlinear control

1. INTRODUCTION

The interest for aerial robots, sometimes called UAVs, UASs, or MAVs, saw a fast improving in the last few years. Indeed, thanks to light-weight and low-cost onboard sensors and computation units, these aerial vehicles became accessible for many companies and robotic labs. A new emerging trend is aerial manipulation in which aerial robots have to physically interact with the environment (Gioioso et al., 2014b; Yüksel et al., 2014; Gioioso et al., 2014a). Nevertheless, some of their typical limitations, such as limited flight time and maximum payload, seriously affect their performances. In particular they could be inapplicable for tasks requiring long time data acquisition or for inspection in the presence of external disturbances like strong wind.

In order to overcome these limitations the tethered solution has been already proposed by several works. In fact the physical link connecting the robot to the ground can be used to provide a constant power supply and a high-bandwidth communication channel, thus improving the flight time and the data transmission. For this system, controllers for the tracking/stabilization of the 2D vertical position of the vehicle while keeping the tether taut have been already presented (Tognon and Franchi, 2017; Lupashin and D'Andrea, 2013; Nicotra et al., 2014). Furthermore, in some of them (Tognon and Franchi, 2017; Lupashin and D'Andrea, 2013) it has been shown that, thanks to the link, an onboard inertial sensor is enough to retrieve the full state of the system wherewith to close the control loop, avoiding the use of GPS or onboard vision.

⋆ This work has been partially funded by the European Union's Horizon 2020 research and innovation programme under grant agreement No 644271 AEROARMS.

It has been also proved that the use of the link can improve the flight stability during risky maneuvers as take-off and landing from a moving platform (Sandino et al., 2014) and a strongly sloped surface (Tognon et al., 2016b), or flight in the presence of strong wind. The use of an actuated winch in order to control the length of the cable was exploited also in (Tognon et al., 2016a) where the problem of controlling the 3D position of an aerial vehicle tethered to a moving platform was addressed. However the use of an actuated winch could be not always the best solution or not even feasible. Indeed it requires a torque controlled motor that increases the mechanics and the electronics of the system, as well as its cost and weight. Moreover, the additional actuation corresponds to an increased controller complexity and of the needed set of sensors.

On the other hand, in this work we analyze a simpler mechatronic system by considering a passive winch applying only a non-controllable (constant) torque, e.g., generated by a spring-based mechanism. This in turn lets reduce the load of the winch itself that could in principle be easily handled by a human being, e.g., in a leash-like configuration. The only controllable actuation is then given by the orientable thrust generated by the underactuated aerial vehicle. In previous works like (Oh et al., 2006; Sandino et al., 2014), where they consider a stabilization problem only for the landing task. Differently in this manuscript we solve the more general exact tracking problem of a desired trajectory for the relative aerial robot position with respect to the platform. To achieve the control objective we prove some intrinsic properties of the system such as exact linearizability through dynamic feedback and differential flatness. Exploiting the first property, we design a nonlinear controller able to exponentially steer the output along the desired trajectory. The second property

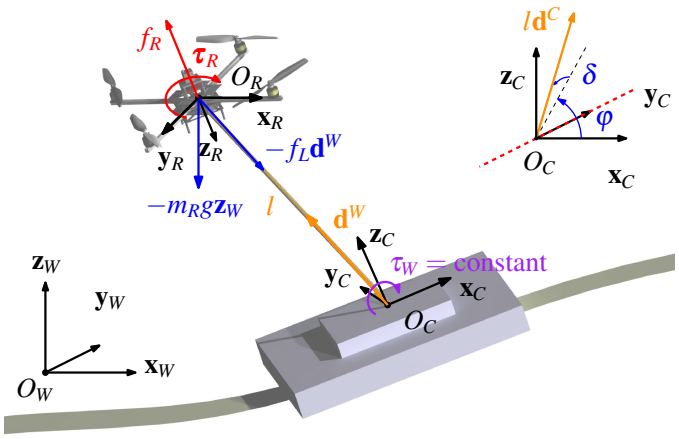

Fig. 1. Left: representation of the system and its main variables. The proposed method works for any VTOL and any independent platform moving generically in 3D. Top right corner: representation of the parametrization of the unit vector $\mathbf{d}^C$. The red line represents the singularities of the link orientation parametrization, which can be avoided in the planning phase.

is instead useful to pre-plan the robot trajectory before tracking it.

The paper is organized as follows. In Sec. 2 the description of the system and its dynamic model are presented. Then in Sec. 3 we prove the exact linearizability of the systems and we design a nonlinear controller for the tracking goal. Sec. 4 presents the proof of the flatness property w.r.t. the output of interest. The designed controller is validated through numerical simulations in Sec. 5. Conclusions and future developments are discussed in Sec. 6.

2. MODELING

In this work we consider a system composed by a *moving platform* that generically moves in the 3D space (e.g., a ground vehicle, a marine vessel or a human operator) and an *aerial vehicle* that is tethered to the moving platform by means of a *link* (e.g., a cable, a rope or a chain). In particular, the link connects the aerial robot to a *passive winch* fixed to the platform. Fig. 1 schematically shows the system and its main variables.

To describe the system we start defining a *world frame*, $\mathcal{F}_W = \{O_W, \mathbf{x}_W, \mathbf{y}_W, \mathbf{z}_W\}$. Then let $\mathcal{F}_C = \{O_C, \mathbf{x}_C, \mathbf{y}_C, \mathbf{z}_C\}$ the *platform frame* rigidly attached to the moving platform with origin O_C expressed by the vector [1] $\mathbf{p}_C^W = [x_C \;\; y_C \;\; z_C]^T \in \mathbb{R}^3$. Similarly, we define $\mathcal{F}_R = \{O_R, \mathbf{x}_R, \mathbf{y}_R, \mathbf{z}_R\}$ as the *aerial vehicle frame*, which is rigidly attached to the aerial vehicle and centered on the center of mass (CoM) of the aerial vehicle. Its position in $\mathcal{F}_W$ is described by the vector $\mathbf{p}_R^W = [x_R \;\; y_R \;\; z_R]^T \in \mathbb{R}^3$.

The configuration of the moving platform is fully given by $\mathbf{p}_C^W$ and $\mathbf{R}_C \in \mathsf{SO}(3)$ (where $\mathsf{SO}(3) = \{\mathbf{A} \in \mathbb{R}^{3\times3} | \mathbf{A}\mathbf{A}^T = \mathbf{I}\}$) describing the orientation of $\mathcal{F}_C$ with respect to $\mathcal{F}_W$. Finally we define $\boldsymbol{\omega}_C \in \mathbb{R}^3$ the angular velocity of $\mathcal{F}_C$ w.r.t. $\mathcal{F}_W$ expressed in $\mathcal{F}_C$. The motion of the moving platform is considered independent from the rest of the system. Indeed in the large majority of the real application scenarios, the aerial system does not influence the platform. In fact the latter has a much larger inertia than the former. On the other hand the aerial vehicle is modeled as a rigid body with mass $m_R \in \mathbb{R}_{>0}$ and positive definite diagonal inertia matrix $\mathbf{J}_R \in \mathbb{R}^{3\times3}$. Its configuration is fully described by $\mathbf{p}_R^W$ and $\mathbf{R}_R \in \mathsf{SO}(3)$. We define $\boldsymbol{\omega}_R \in \mathbb{R}^3$ the angular velocity of $\mathcal{F}_R$ w.r.t. $\mathcal{F}_W$ expressed in $\mathcal{F}_R$. The motion of the vehicle is controlled by $f_R \in \mathbb{R}$, the intensity of the thrust force $\mathbf{f}_R = -f_R\mathbf{z}_R$ applied at O_R, and by $\boldsymbol{\tau}_R = [\tau_{Rx} \;\; \tau_{Ry} \;\; \tau_{Rz}]^T \in \mathbb{R}^3$, the input torque vector expressed in $\mathcal{F}_R$.

The link is connected to one side to the aerial vehicle at O_R by a passive 3D rotational joint, and to the other side to the platform at O_C, by means of the passive winch. As done in related previous works (Oh et al., 2006) we assume the mass and the inertia of the link negligible with respect to the one of the aerial vehicle, and deformation and elasticity effects negligible as well. These assumptions have been strongly validated in practice (Tognon et al., 2016b). The orientation of the link is given by the unit vector $\mathbf{d}^C \in \mathsf{S}^2$ expressed in $\mathcal{F}_C$ (where $\mathsf{S}^2 = \{\mathbf{v} \in \mathbb{R}^3 | \, \|\mathbf{v}\| = 1\}$). Finally we define its length $l \in \mathbb{R}_{>0}$ and the *internal force* $f_L \in \mathbb{R}$ along it. To keep the link taut the internal force has to be always positive (in this case it is called *tension*). We choose to parametrize $\mathbf{d}^C$ by the angles *elevation*, $\varphi \in [0, 2\pi]$, and *azimuth*, $\delta \in [-\pi/2, \pi/2]$, as

$$\mathbf{d}^C = [\cos\delta\cos\varphi \quad -\sin\delta \quad \cos\delta\sin\varphi]^T .$$

This is not the usual spherical parametrization (see Fig. 1). In this way we move the singularity from the axis $\mathbf{z}_C$ for the standard spherical parametrization, that is a frequent condition during operations, to the axis $\mathbf{y}_C$.

The passive winch is modeled as a cylinder where the link is winded up or out, with inertia $J_W \in \mathbb{R}_{>0}$ and radius $r_W \in \mathbb{R}_{>0}$ [2], fixed to the platform in the proximity of O_C. Its rotation angle is described by the variable $\vartheta_W \in \mathbb{R}$. The winch is passive because a non-controllable constant torque $\tau_W \in \mathbb{R}$ is applied along the longitudinal axis of the cylinder, e.g., generated by a simple constant torque spring. The length l can be then controlled only by the action of the thrust provided by the aerial vehicle.

The choice of a passive winch instead of a controllable winch makes the system and easily portable by an human operator. On the other hand, as it will be clear in Sec. 3, the price to pay will be a reduced control authority on the variables of the system with respect to the case with a controllable winch. In particular, the tension of the link cannot be regulated to an arbitrary value while following a position trajectory. However it can be maintained within a desired bound, if the desired trajectory is well planned.

Considering the constraints of the system, the rotational dynamics of the aerial vehicle appears to be independent to the translational one. Hence it is given by:

$$\dot{\mathbf{R}}_R = \mathbf{R}_R\boldsymbol{\Omega}_R \tag{1}$$

$$\mathbf{J}_R\dot{\boldsymbol{\omega}}_R = \mathbf{J}_R\boldsymbol{\omega}_R \times \boldsymbol{\omega}_R + \boldsymbol{\tau}_R, \tag{2}$$

where [3] $\boldsymbol{\Omega}_R = [\boldsymbol{\omega}_R]_\times$. On the other hand, considering the motion of the moving platform as a measured exogenous input, the translation dynamics of the aerial vehicles is described by the generalized coordinates $\mathbf{q} = [l \;\; \varphi \;\; \delta]^T$. The dynamics is derived applying the Lagrangian approach as

[1] In this work, the superscript indicates the frame of references.

[2] For simplicity, J_W and r_W are assumed constant independently from the amount of link that is winded-up. However the model is easily extendable if needed.

[3] The operator $[\mathbf{v}]_\times$ for any vector $\mathbf{v} \in \mathbb{R}^3$, returns the skew symmetric matrix such that $[\mathbf{v}]_\times \mathbf{w} = \mathbf{v} \times \mathbf{w}$ for any $\mathbf{w} \in \mathbb{R}^3$.

$$\mathbf{M}\ddot{\mathbf{q}} + \mathbf{c} + \mathbf{g} + \mathbf{n} + \mathbf{w} = \mathbf{Q}\mathbf{u} \tag{3}$$

where $\mathbf{M}(\mathbf{q}) \in \mathbb{R}^{3\times3}$ is the positive definite inertia matrix, $\mathbf{c}(\mathbf{q}, \dot{\mathbf{q}}, \dot{\mathbf{p}}_C^C, \boldsymbol{\omega}_C) \in \mathbb{R}^3$ contains all the centrifugal/Coriolis terms, $\mathbf{g}(\mathbf{q}, \mathbf{R}_C) \in \mathbb{R}^3$ contains all the gravity terms, $\mathbf{n}(\mathbf{q}, \ddot{\mathbf{p}}_C^C, \dot{\boldsymbol{\omega}}_C) \in \mathbb{R}^3$ contains the terms depending on the acceleration of the moving platform, $\mathbf{w}(\tau_W) \in \mathbb{R}^3$ contains the terms depending on the constant torque winch, and $\mathbf{Q}(\mathbf{q}, \mathbf{R}_R, \mathbf{R}_C) \in \mathbb{R}^{3\times4}$ is related to the generalized forces, referred as $\mathbf{a_u}$, performing work on $\mathbf{q}$, such that

$$\mathbf{a_u} = \mathbf{Q}(\mathbf{q}, \mathbf{R}_R, \mathbf{R}_C)\mathbf{u} = [-\mathbf{J}_\mathbf{q}^T\mathbf{R}_C^T\mathbf{R}_R\mathbf{e}_3 \;\; \mathbf{0}_{3\times3}]\mathbf{u},$$

where $\mathbf{J_q} = \frac{\partial \mathbf{p}_R^C}{\partial \mathbf{q}} \in \mathbb{R}^{3\times3}$ is the Jacobian matrix of $\mathbf{p}_R^C$, and $\mathbf{u} = [u_1 \;\; \mathbf{u}_2^T]^T = [f_R \;\; \boldsymbol{\tau}_R^T]^T \in \mathbb{R}^4$ is the input vector. For space limitation we do not report here the full expression of each term. The state of the system is then expressed by $\mathbf{x} = (\mathbf{q}, \dot{\mathbf{q}}, \mathbf{R}_R, \boldsymbol{\omega}_R)$. Finally, to complete the characterization of the system, we derive the link internal force from the balance of momenta on the winch along its longitudinal axis:

$$f_L = \bar{J}_W\ddot{l} - \bar{\tau}_W, \tag{4}$$

where $\bar{J}_W = J_W/r_W^2$ and $\bar{\tau}_W = \tau_W/r_W$.

The problems addressed in this work are the following.

Problem 1. Design a control law for the inputs f_R and $\boldsymbol{\tau}_R$ to let $\mathbf{q}$ (or equivalently $\mathbf{p}_R^C$ thanks to inverse kinematics) exactly track any sufficiently smooth desired trajectory.

Problem 2. Given the desired trajectory of $\mathbf{q}$, define a method to compute the nominal state and input in order to obtain the tracking of the desired trajectory.

The first objective allows to control the relative position of the aerial vehicle with respect to the moving platform, while the second can be exploited in a planning phase to design a desired trajectory that fulfills input limitations or that keeps the internal force bounded (see Sec. 4.1).

3. DYNAMIC DECOUPLING CONTROL

Define as output of interest the quantity $\mathbf{y_q} = [y_1 \;\; y_2 \;\; y_3]^T = \mathbf{q} \in \mathbb{R}^3$. Although the dimension of $\mathbf{u}$ is greater than the the dimension of $\mathbf{y_q}$, the control problem is not redundant because τ_{Rz} neither affects $\mathbf{y_q}$ nor its derivatives. Indeed τ_{Rz} does not change the thrust vector direction, $\mathbf{f}_R$, that is the only quantity that, together with τ_W, plays a role in the dynamics of $\mathbf{y_q}$. To obtain a well posed tracking problem we have to complete the set of outputs with a quantity dynamically dependent on τ_{Rz}. For this purpose we can consider any generic parametrization $\boldsymbol{\eta} = [\eta_1 \;\; \eta_3 \;\; \eta_3]^T \in \mathbb{R}^3$ of $\mathbf{R}_R$, such that $\mathbf{R}_R = \mathbf{R}_R(\boldsymbol{\eta})$ and $\dot{\boldsymbol{\eta}} = \mathbf{T}_{\boldsymbol{\eta}}\boldsymbol{\omega}_R$, where $\mathbf{T}_{\boldsymbol{\eta}}(\boldsymbol{\eta}) \in \mathbb{R}^{3\times3}$ is given by the particular parametrization. From (2) the dynamics of $\boldsymbol{\eta}$ is

$$\begin{aligned}\ddot{\boldsymbol{\eta}} &= \dot{\mathbf{T}}_{\boldsymbol{\eta}}\boldsymbol{\omega}_R + \mathbf{T}_{\boldsymbol{\eta}}\mathbf{J}_R^{-1}(\mathbf{J}_R\boldsymbol{\omega}_R \times \boldsymbol{\omega}_R) + [\mathbf{0}_{3\times1} \;\; \mathbf{T}_{\boldsymbol{\eta}}\mathbf{J}_R^{-1}]\mathbf{u} \\ &= \mathbf{b}_{\boldsymbol{\eta}}(\boldsymbol{\eta}, \dot{\boldsymbol{\eta}}) + \mathbf{E}_{\boldsymbol{\eta}}(\boldsymbol{\eta})\mathbf{u}.\end{aligned} \tag{5}$$

Then we consider $y_4 = \eta_i$, where η_i is any entry of $\boldsymbol{\eta}$, as additional angle that is dynamically dependent from τ_{Rz}, i.e., such that

$$\partial\ddot{\eta}_i/\partial\tau_{Rz} = \mathbf{e}_i^T\mathbf{T}_{\boldsymbol{\eta}}\mathbf{J}_R^{-1}\mathbf{e}_3 \neq 0. \tag{6}$$

Considering $\mathbf{y} = [\mathbf{y_q}^T \;\; y_4]^T$ as output of interest and applying the feedback linearization technique, we need to differentiate each entry of $\mathbf{y}$ until the input appears. From equations (3) and (5), $\mathbf{y}$ has to be differentiated twice to see the input appear:

$$\begin{aligned}\begin{bmatrix}\ddot{\mathbf{y}}_\mathbf{q} \\ \ddot{y}_4\end{bmatrix} &= \begin{bmatrix}\bar{\mathbf{M}}\mathbf{a} \\ b_{\eta_i}\end{bmatrix} + \begin{bmatrix}\bar{\mathbf{M}}\mathbf{Q} \\ \mathbf{e}_{\eta_i}\end{bmatrix}\mathbf{u} \\ &= \begin{bmatrix}\bar{\mathbf{M}}\mathbf{a} \\ b_{\eta_i}\end{bmatrix} + \begin{bmatrix}-\mathbf{J}_\mathbf{q}^T\mathbf{R}_C^T\mathbf{R}_R\mathbf{e}_3 & \mathbf{0}_{3\times3} \\ 0 & \mathbf{e}_i^T\mathbf{T}_{\boldsymbol{\eta}}\mathbf{J}_R^{-1}\end{bmatrix}\mathbf{u} \\ &= \mathbf{b}(\mathbf{x}, \mathbf{X}_C^2) + \mathbf{E}(\mathbf{x}, \mathbf{X}_C^0)\mathbf{u},\end{aligned} \tag{7}$$

where $\bar{\mathbf{M}} = \mathbf{M}^{-1}$, $b_{\eta_i} = \mathbf{e}_i^T\mathbf{b}_{\boldsymbol{\eta}}$, $\mathbf{e}_{\eta_i} = \mathbf{e}_i^T\mathbf{E}_{\boldsymbol{\eta}}$, $\mathbf{a} = -\mathbf{c} - \mathbf{g} - \mathbf{n} - \mathbf{w}$, and $\mathbf{X}_C^j = (\mathbf{x}_C^0, \mathbf{x}_C^1, \ldots, \mathbf{x}_C^j)$ for $j \in \mathbb{N}^+$, $\mathbf{x}_C^i = (\mathbf{p}_C^{C(i)}, \boldsymbol{\omega}_C^{(i-1)})$ for $i = 1, 2, \ldots$. The decoupling matrix $\bar{\mathbf{E}}$ is singular for every condition because $\boldsymbol{\tau}_R$ does not appear on $\mathbf{y_q}$. This means that the system is not statically feedback linearizable.

In this case one can apply a dynamic feedback inserting a dynamic compensator in the control u_1. Consider as new input the second derivative of the thrust and the torque, i.e., $\bar{\mathbf{u}} = [\ddot{u}_1 \;\; \mathbf{u}_2^T]^T$. Now $\mathbf{y_q}$ has to be differentiated four times to see $\bar{\mathbf{u}}$ appear, while for y_4 everything remains the same, indeed:

$$\begin{bmatrix}\mathbf{y}_\mathbf{q}^{(4)} \\ \ddot{y}_4\end{bmatrix} = \begin{bmatrix}\ddot{\bar{\mathbf{M}}}(\mathbf{a} + \mathbf{a_u}) + 2\dot{\bar{\mathbf{M}}}(\dot{\mathbf{a}} + \dot{\mathbf{a}}_\mathbf{u}) + \bar{\mathbf{M}}(\ddot{\mathbf{a}} + \ddot{\mathbf{a}}_\mathbf{u}) \\ b_i + \mathbf{e}_{\eta_i}\bar{\mathbf{u}}\end{bmatrix}, \tag{8}$$

where $\ddot{\mathbf{a}}_\mathbf{u}$, after replacing the system dynamics, results:

$$\ddot{\mathbf{a}}_\mathbf{u} = \bar{\ddot{\mathbf{a}}}_\mathbf{u} + \mathbf{J}_\mathbf{q}^T\mathbf{R}_C^T\mathbf{R}_R(-\ddot{u}_1\mathbf{e}_3 - u_1\left[\mathbf{J}_R^{-1}\boldsymbol{\tau}_R\right]_\times\mathbf{e}_3), \tag{9}$$

where $\bar{\ddot{\mathbf{a}}}_\mathbf{u}$ gathers all the terms that do not depend on $\bar{\mathbf{u}}$. Since $\mathbf{J}_R$ is diagonal, writing the skew symmetric matrix relative to $\mathbf{J}_R^{-1}\boldsymbol{\tau}_R$ and doing some algebra we obtain

$$\left[\mathbf{J}_R^{-1}\boldsymbol{\tau}_R\right]_\times\mathbf{e}_3 = \begin{bmatrix}-\dfrac{\mathbf{e}_2}{J_{R11}} & \dfrac{\mathbf{e}_1}{J_{R22}} & \mathbf{0}_{3\times1}\end{bmatrix}\boldsymbol{\tau}_R, \tag{10}$$

where J_{Rkm} corresponds to the element of the matrix $\mathbf{J}_R$ in the position k, m. Replacing equations (10) and (9) into (8) we obtain

$$\begin{bmatrix}\mathbf{y}_\mathbf{q}^{(4)} \\ \ddot{y}_4\end{bmatrix} = \bar{\mathbf{b}}(\bar{\mathbf{x}}, \mathbf{X}_C^4) + \underbrace{\begin{bmatrix}\bar{\mathbf{M}}\mathbf{J}_\mathbf{q}^T\mathbf{R}_C^T\mathbf{R}_R\mathbf{T} & \mathbf{0}_{3\times1} \\ \tilde{\mathbf{e}}_3 & \tilde{e}_2\end{bmatrix}}_{\bar{\mathbf{E}}(\bar{\mathbf{x}}, \mathbf{X}_C^0)}\bar{\mathbf{u}},$$

where, $\bar{\mathbf{x}} = (\mathbf{q}, \dot{\mathbf{q}}, \mathbf{R}_R, \boldsymbol{\omega}_R, f_R, \dot{f}_R)$ is the extended state, $\bar{\mathbf{b}}(\bar{\mathbf{x}}, \mathbf{X}_C^4)$ collects all the terms that do not depend on $\bar{\mathbf{u}}$, $\mathbf{T} = [\mathbf{e}_3 \;\; -\frac{u_1}{J_{R11}}\mathbf{e}_2 \;\; \frac{u_1}{J_{R22}}\mathbf{e}_1]$, $\tilde{e}_2 = \mathbf{e}_i^T\mathbf{T}_{\boldsymbol{\eta}}\mathbf{J}_R^{-1}\mathbf{e}_3$, and $\tilde{\mathbf{e}}_3 = \mathbf{e}_i^T\mathbf{T}_{\boldsymbol{\eta}}\mathbf{J}_R^{-1}[\mathbf{0}_{3\times1} \;\; \mathbf{e}_1 \;\; \mathbf{e}_2]$. The decoupling matrix $\bar{\mathbf{E}}$ results to be invertible if $\tilde{e}_2 \neq 0$ and if $\mathbf{T}$ is invertible, since $\mathbf{R}_R$, $\mathbf{R}_C$, $\mathbf{J_q}$ and $\bar{\mathbf{M}}$ are always full rank (except where the model is singular, i.e., for $l = 0$ or $\delta = \pm\pi/2$). Thus it is easy to verify that $\bar{\mathbf{E}}$ is invertible if $u_1 \neq 0$ and if the parametrization $\boldsymbol{\eta}$ of $\mathbf{R}_R$ and one of its elements η_i are chosen such that $\tilde{e}_2 \neq 0$, i.e., if (6) is verified in the domain of interest.

Then, in the case in which $\bar{\mathbf{E}}$ is invertible, defining $\mathbf{v} = [v_1 \;\; v_2 \;\; v_3 \;\; v_4]^T \in \mathbb{R}^4$ as virtual inputs, the control law

$$\bar{\mathbf{u}} = \bar{\mathbf{E}}(\bar{\mathbf{x}}, \mathbf{X}_C^0)^{-1}\left[-\bar{\mathbf{b}}(\bar{\mathbf{x}}, \mathbf{X}_C^4) + \mathbf{v}\right], \tag{11}$$

brings the original system in the equivalent linear system:

$$y_1^{(4)} = v_1, \quad y_2^{(4)} = v_2, \quad y_3^{(4)} = v_3, \quad y_4^{(2)} = v_4. \tag{12}$$

This means that the system results to be exactly linearizable through dynamic feedback and the linearized system (12) does not have an internal dynamics. Indeed,

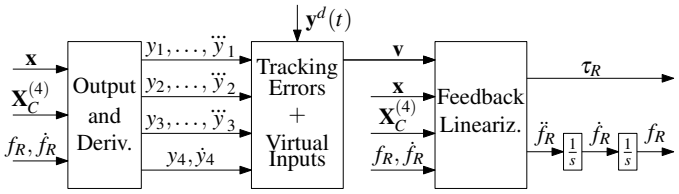

Fig. 2. Graphic representation of the control strategy. Notice that the inputs of the controller are only the state of the system, $\mathbf{x}$, the informations related to the motion of the platform, $\mathbf{X}_C^4$, and the state of the controller itself, f_R and $\dot{f}_R$.

the total relative degree [4] with respect to $\mathbf{y}$ is $r = 4 + 4 + 4 + 2 = 14 = \bar{n}$, where $\bar{n}$ is dimension of the extended state $\bar{\mathbf{x}}$. Considering (12), one can apply any linear control technique to achieve the tracking of the desired trajectories $y_i^d(t) \in C^3$ for $i = 1, 2, 3$ and $y_4^d(t) \in C^1$, e.g., a pole placing based controller:

$$v_i = y_i^{d(4)} + \mathbf{k}_i^T \boldsymbol{\xi}_i, \qquad v_4 = y_4^{d(2)} + \mathbf{k}_4^T \boldsymbol{\xi}_4 \tag{13}$$

where $\boldsymbol{\xi}_i = [\xi_i^{(3)} \;\; \ddot{\xi}_i \;\; \dot{\xi}_i \;\; \xi_i]^T \in \mathbb{R}^4$, $\boldsymbol{\xi}_4 = [\dot{\xi}_4 \;\; \xi_4]^T \in \mathbb{R}^2$, $\xi_i = y_i^d - y_i$ and $\xi_4 = y_4^d - y_4$ are the tracking errors. The gains $\mathbf{k}_i \in \mathbb{R}^4_{>0}$ for $i = 1, 2, 3$, and $\mathbf{k}_4 \in \mathbb{R}^2_{>0}$, set the poles of the closed loop system. A block diagram of the proposed control method is showed in Fig. 2.

Proposition 1. Consider the system composed by an underactuated aerial vehicle tethered by a link to a passive winch (i.e., pulling the link with a constant, uncontrollable, torque) fixed on a moving platform. Then, it exists at least one parametrization $\boldsymbol{\eta}$ of $\mathbf{R}_R$ and one of its elements η_i, such that $\mathbf{y} = [l \;\; \varphi \;\; \delta \;\; \eta_i]^T$ is an exact feedback linearizing output for each state, except when the total thrust is zero. In fact, if $f_R \neq 0$, the dynamic feedback transformation (11) brings the original nonlinear system (1), (2) and (3), into a fully-equivalent linear and decoupled dynamical system for every state configuration. Furthermore, considering as input $\bar{\mathbf{u}}$, the control laws (11) and (13) exponentially steer $\mathbf{y}$ along the desired trajectories $y_i^d(t) \in C^3$ for $i = 1, 2, 3$, and $y_4^d(t) \in C^1$.

4. DIFFERENTIAL FLATNESS

To achieve the second objective we shall prove the *differential flatness* of the system with respect to the output $\mathbf{y}$. In other words we show that the state and the input of the system can be written as algebraic function of the output and a finite number of its derivatives (Fliess et al., 1995). Thus, given the desired trajectory of the output one can compute the nominal state and inputs needed to follow the desired trajectory. This property is useful for planning and optimization in order to generate feasible trajectories under input limitations or other constraints on the state.

It has been proved that an exactly dynamical feedback linearizing output is also a flat output on an open and dense set of the state space (De Luca and Oriolo, 2002). This means that since the system is dynamic feedback linearizable, it is also differential flat. Nevertheless, it is useful to provide the explicit expression of $\mathbf{x}$ and $\mathbf{u}$ as function of $\mathbf{y}$ and its derivatives when η_i is the yaw angle.

Part of the state is directly given by $\mathbf{y_q}$, i.e., $\mathbf{q} = \mathbf{y_q}$, $\dot{\mathbf{q}} = \dot{\mathbf{y}}_\mathbf{q}$. Only the part of the state related to the rotational dynamics and the inputs have still to be derived. From (4) we can write the internal force as function of $\ddot{\mathbf{y}}_\mathbf{q}$:

$$f_L = \bar{J}_W \ddot{l} - \bar{\tau}_W = f_L(\ddot{\mathbf{y}}_\mathbf{q}). \tag{14}$$

We can also write $\mathbf{d}^C$ and $\mathbf{J_q}$ as function of the output, i.e., $\mathbf{d}^C = \mathbf{d}^C(\mathbf{y_q})$ and $\mathbf{J_q} = \mathbf{J_q}(\mathbf{y_q})$. Then, if the linear velocity, the attitude of the platform and their time derivatives are known, we can write $\ddot{\mathbf{p}}_R^W$ as function of $\mathbf{y_q}$, $\dot{\mathbf{y}}_\mathbf{q}$ and $\ddot{\mathbf{y}}_\mathbf{q}$, as

$$\begin{aligned}\ddot{\mathbf{p}}_R^W &= \mathbf{R}_C[\boldsymbol{\Omega}_C(\dot{\mathbf{p}}_C^C + l\boldsymbol{\Omega}_C\mathbf{d}^C(\mathbf{y_q}) + 2\mathbf{J_q}(\mathbf{y_q})\dot{\mathbf{y}}_\mathbf{q}) + \ddot{\mathbf{p}}_C^C + \\ &\quad + l\dot{\boldsymbol{\Omega}}_C\mathbf{d}^C(\mathbf{y_q}) + \dot{\mathbf{J}}_\mathbf{q}(\mathbf{y_q}, \dot{\mathbf{y}}_\mathbf{q})\dot{\mathbf{y}}_\mathbf{q} + \mathbf{J_q}(\mathbf{y_q})\ddot{\mathbf{y}}_\mathbf{q}] \\ &= \ddot{\mathbf{p}}_R^W(\mathbf{y_q}, \dot{\mathbf{y}}_\mathbf{q}, \ddot{\mathbf{y}}_\mathbf{q}, \mathbf{X}_C^2).\end{aligned}$$

Writing the force balance equation at O_R we can retrieve the thrust vector as function of $\mathbf{y_q}$ and its derivatives, as

$$\begin{aligned}\mathbf{f}_R &= -m_R\ddot{\mathbf{p}}_R^W(\mathbf{y_q}, \dot{\mathbf{y}}_\mathbf{q}, \ddot{\mathbf{y}}_\mathbf{q}, \mathbf{X}_C^2) - f_L(\ddot{\mathbf{y}}_\mathbf{q})\mathbf{R}_C\mathbf{d}^C(\mathbf{y_q}) \\ &\quad - m_R g\mathbf{e}_3 = \mathbf{f}_R(\mathbf{y_q}, \dot{\mathbf{y}}_\mathbf{q}, \ddot{\mathbf{y}}_\mathbf{q}, \mathbf{X}_C^2).\end{aligned}$$

From the previous equation, in order to find the missing states, $\mathbf{R}_R$ and $\boldsymbol{\omega}_R$, and the inputs, f_R and $\boldsymbol{\tau}_R$, in function of $\mathbf{y}$ and its derivatives, one can use the same method in (Mellinger and Kumar, 2011). We do not report here the explicit derivation for space limitation.

Proposition 2. The model (1), (2) and (3), is differentially flat with respect to the flat outputs $\mathbf{y} = [l \;\; \varphi \;\; \delta \;\; \eta_i]^T$ where η_i is the yaw angle of $\mathbf{R}_R$. In other words the state and the inputs can be written as algebraic function of $\mathbf{y}$ and a finite number of its derivatives.

4.1 Discussion on Link Internal Force Regulation

Notice that, differently from previous related works such as (Tognon and Franchi, 2017; Tognon et al., 2016a), the internal force along the link is not part of the flat output for this system. This means that its value can not be directly controlled. On the contrary, from (14), it is a byproduct of the desired output trajectory, and in particular of the desired link length acceleration. Nevertheless, in order to keep the internal force always positive and within a desired bound $\mathcal{B}_{f_L} = [\underline{f_L}, \overline{f_L}]$ where $\underline{f_L}, \overline{f_L} \in \mathbb{R}_{\geq 0}$, we can exploit the flatness of the system to design suitable desired trajectories of $\mathbf{y}$. In particular, from equation (14) we have that $f_L \in \mathcal{B}_{f_L}$ if and only if $\ddot{l} \in \mathcal{B}_{\ddot{l}} = [\underline{\ddot{l}}, \overline{\ddot{l}}]$ where $\overline{\ddot{l}} = (\bar{\tau}_W + \overline{f_L})/\bar{J}_W$ and $\underline{\ddot{l}} = (\bar{\tau}_W + \underline{f_L})/\bar{J}_W$. In other words the constraint on the internal force can be translates by the flatness to a constraint on the desired trajectory of l.

Notice that the steady configuration, $\ddot{l} = 0$, belongs to $\mathcal{B}_{\ddot{l}}$ if and only if $\underline{\ddot{l}} \leq 0 \leq \overline{\ddot{l}}$ that in turn means $-\overline{f_L} \leq \bar{\tau}_W \leq -\underline{f_L}$. In particular, if for $\ddot{l} = 0$ we wants a particular internal force value ${f_L}^\star \in \mathcal{B}_{f_L}$, we have to design the passive winch such that $\bar{\tau}_W = \tau_W / r_W = -{f_L}^\star$. Another parameter of the winch that can be optimized is it inertia $\bar{J}_W$. Indeed it affects how $\mathcal{B}_{f_L}$ is mapped on $\mathcal{B}_{\ddot{l}}$, e.g., if we make $\bar{J}_W$ small enough, big variations of $\ddot{l}$ imply small variations of the internal force and thus an almost constant internal force, $f_L \approx {f_L}^\star$.

5. NUMERICAL VALIDATION

Through numerical simulation we shall validate our control method showing that the output of interest exponentially

[4] i.e., the sum, for each element of the output, of the number of times that each output entry has to be differentiated in order to see the input appear.

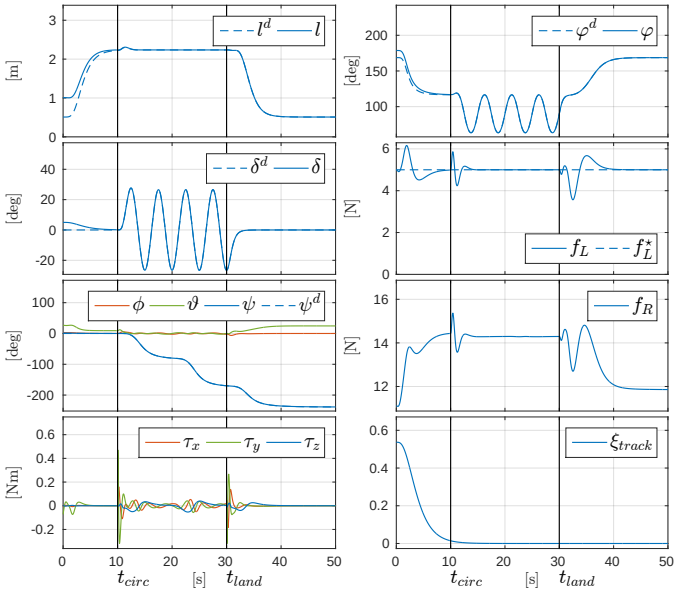

Fig. 3. Simulation results with an initial tracking error (case a).

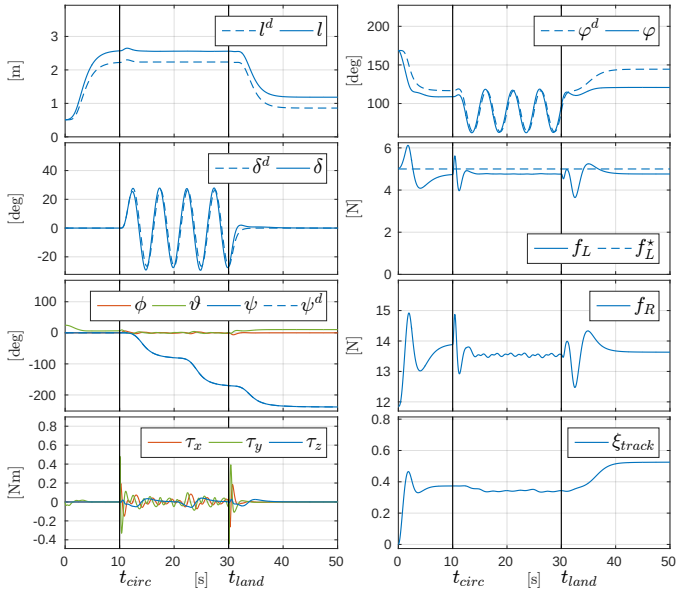

Fig. 4. Simulation results with parameters uncertainties (case b). The steady state error can be removed with any robustifying action such as an integral term in the outer loop.

converges to the desired trajectory in case of initial error, as well as it shows good tracking performances in several non-ideal conditions.

We consider an aerial vehicle of mass $m_R = 1\,[\text{kg}]$ and inertia $\mathbf{J}_R = 0.25\mathbf{I}_3\,[\text{kg}\cdot\text{m}^2]$, where $\mathbf{I}_3 \in \mathbb{R}^{3\times3}$ is the identity matrix. The winch has a constant radius $r_W = 0.2\,[\text{m}]$ and a constant inertia $J_W = 0.15\,[\text{kg}\cdot\text{m}^2]$. In order to obtain a steady state internal force ${f_L}^\star = 5\,[\text{N}]$, we set the torque winch $\tau_W = -1\,[N]$ (see Sec. 4.1). Finally, to obtain a sufficiently fast exponentially tracking, we set the controller gains $\mathbf{k}_i$ and $\mathbf{k}_4$ such that the error dynamics ξ_i and ξ_4 have poles in $(-0.5, -1, -1.5, -2)$ and $(-0.5, -1)$, respectively, for $i = 1, 2, 3$.

We design the platform motion and the aerial vehicle desired trajectory in order to simulate a patrol-like task of a delimited area. The platform simply travel the perimeter of the area of interest while the aerial vehicle, after the take-off maneuver, at time t_{circ} has to loiter above the platform. Then, starting from time t_{land} the aerial vehicle has to land on the platform. The trajectories of the systems are plotted in Fig. 5b. Notice that take-off and landing are performed while the platform is moving, making these standard maneuvers non trivial.

To validate the control method and to test its robustness we performed several simulations in different non ideal conditions: a) initial tracking error, b) variation of the model parameters, c) noise on the measured state used for the feedback. d) non ideal motor modeled as a first order system characterized by a certain time constant.

Case a): we initialized the system with an initial tracking error of $10\,[°]$ for the elevation, of $5\,[°]$ for the azimuth and of $0.5\,[\text{m}]$ for the link length. Looking at Fig. 3 we can notice that after a transient, the controller steers the output of interest along the desired trajectory. Notice that the internal force along the link remains always positive and close to the desired steady state value ${f_L}^\star$. Furthermore it is exactly equal to ${f_L}^\star$ whenever $\ddot{l}$ is zero.

Case b): in a real implementation it is very unluckily to have a perfect knowledge of the model and its parameters. For this reason we tested the robustness of the control method with a variation of the 5% on all the model's parameters (see Fig. 4). Due to the mismatch between real and nominal model, the feedback linearization is not exact and the error does not go to zero. However it remains always bounded showing nicely degrading and sufficiently good tracking performances. With further simulations we noticed that the system remains stable showing acceptable tracking errors up to a parametric variation of 50%, proving the robustness of the proposed method. Above the system becomes unstable.

Case c): we tested the robustness of the proposed method injecting Gaussian noise on the measured state used to close the control loop. The power of the noise has the same value of the one noticed in (Tognon et al., 2016a) out of an observer based on noisy sensors. From Fig. 5 one can see that the error does not converge to zero but remains always bounded showing good and practically viable tracking performances.

Case d): in this simulation we considered the thrust and the toque of the aerial vehicle generated by non-ideal motors modeled as a first order system characterized by a time constant of 0.2 [s]. The results displayed in Fig. 6 show a very small tracking error, validating the robustness of the control method to this additional non-ideality.

6. CONCLUSIONS

In this manuscript we faced the problem concerning an aerial vehicle moving in the 3D space, tethered to a passive winch rigidly attached to an independently moving platform. For this robotic system we went beyond the simple regulation problem proposing a nonlinear tracking controller able to let the aerial robot position follow any sufficiently smooth time-varying trajectory, while the platform is moving. The proposed method can then be applied for application such as inspection or data acquisition, as shown in simulation in different non-ideal conditions as well. The validation of the method with real experiment in a plausible scenario is left for future works, e.g., with minimalistic and onboard sensor settings (Franchi et al.,

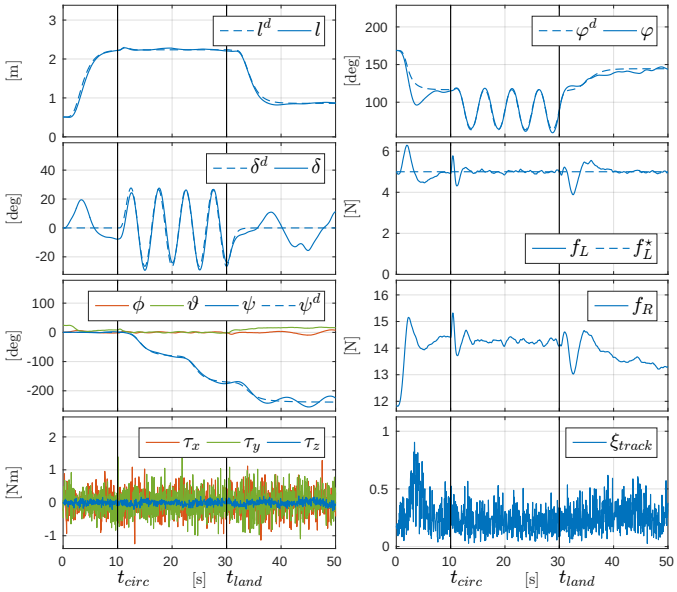

(a) Controller performances: the tracking of the output of interest is plotted.

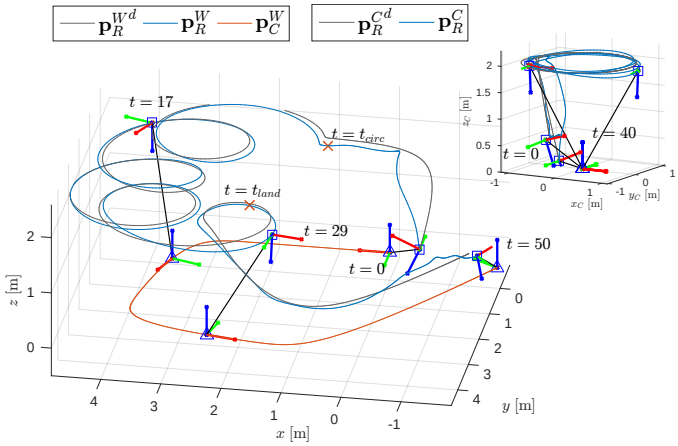

(b) Trajectories visualization. Left: trajectories in the world frame. Right: aerial vehicle trajectory in the moving platform frame. Red line: platform trajectory. Blue line: aerial robot trajectory

Fig. 5. Simulation results with additional noise on the state.

2013; Stegagno et al., 2014), as well as an improvement and full development of a trajectory planning method.

REFERENCES

De Luca, A. and Oriolo, G. (2002). Trajectory planning and control for planar robots with passive last joint. *The International Journal of Robotics Research*, 21(5-6), 575–590.

Fliess, M., Lévine, J., Martin, P., and Rouchon, P. (1995). Flatness and defect of nonlinear systems: Introductory theory and examples. *International Journal of Control*, 61(6), 1327–1361.

Franchi, A., Oriolo, G., and Stegagno, P. (2013). Mutual localization in multi-robot systems using anonymous relative measurements. *The International Journal of Robotics Research*, 32(11), 1302–1322.

Gioioso, G., Franchi, A., Salvietti, G., Scheggi, S., and Prattichizzo, D. (2014a). The Flying Hand: a formation of UAVs for cooperative aerial tele-manipulation. In *2014 IEEE Int. Conf. on Robotics and Automation*, 4335–4341. Hong Kong, China.

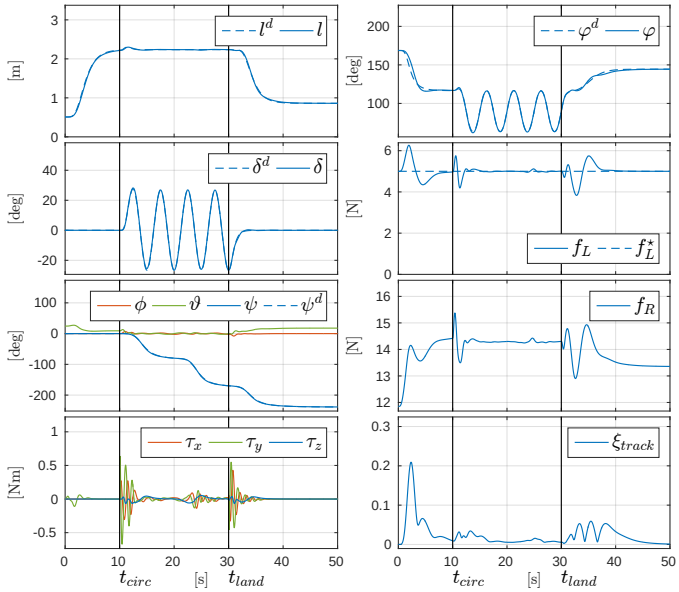

Fig. 6. Simulation results of a plausible task trajectory with non ideal motors characterized by a time constant equal to 0.2 [s].

Gioioso, G., Ryll, M., Prattichizzo, D., Bülthoff, H.H., and Franchi, A. (2014b). Turning a near-hovering controlled quadrotor into a 3D force effector. In *2014 IEEE Int. Conf. on Robotics and Automation*, 6278–6284. Hong Kong, China.

Lupashin, S. and D'Andrea, R. (2013). Stabilization of a flying vehicle on a taut tether using inertial sensing. In *2013 IEEE/RSJ Int. Conf. on Intelligent Robots and Systems*, 2432–2438. Tokyo, Japan.

Mellinger, D. and Kumar, V. (2011). Minimum snap trajectory generation and control for quadrotors. In *2011 IEEE Int. Conf. on Robotics and Automation*, 2520–2525. Shanghai, China.

Nicotra, M.M., Naldi, R., and Garone, E. (2014). Taut cable control of a tethered UAV. In *19th IFAC World Congress*, 3190–3195. Cape Town, South Africa.

Oh, S.R., Pathak, K., Agrawal, S.K., Pota, H.R., and Garrett, M. (2006). Approaches for a tether-guided landing of an autonomous helicopter. *IEEE Trans. on Robotics*, 22(3), 536–544.

Sandino, L., Santamaria, D., Bejar, M., Viguria, A., Kondak, K., and Ollero, A. (2014). Tether-guided landing of unmanned helicopters without GPS sensors. In *2014 IEEE Int. Conf. on Robotics and Automation*, 3096–3101. Hong Kong, China.

Stegagno, P., Basile, M., Bülthoff, H.H., and Franchi, A. (2014). A semi-autonomous UAV platform for indoor remote operation with visual and haptic feedback. In *2014 IEEE Int. Conf. on Robotics and Automation*, 3862–3869. Hong Kong, China.

Tognon, M., Dash, S.S., and Franchi, A. (2016a). Observer-based control of position and tension for an aerial robot tethered to a moving platform. *IEEE Robotics and Automation Letters*, 1(2), 732–737.

Tognon, M. and Franchi, A. (2017). Dynamics, control, and estimation for aerial robots tethered by cables or bars. *IEEE Trans. on Robotics*.

Tognon, M., Testa, A., Rossi, E., and Franchi, A. (2016b). Takeoff and landing on slopes via inclined hovering with a tethered aerial robot. In *2016 IEEE/RSJ Int. Conf. on Intelligent Robots and Systems*, 1702–1707. Daejeon, South Korea.

Yüksel, B., Secchi, C., Bülthoff, H.H., and Franchi, A. (2014). Reshaping the physical properties of a quadrotor through IDA-PBC and its application to aerial physical interaction. In *2014 IEEE Int. Conf. on Robotics and Automation*, 6258–6265. Hong Kong, China.